


Minoxidil Cannot Be Used To Target Lysyl Hydroxylases during Postnatal Mouse Lung Development: A Cautionary Note[§]

Tilman Pfeffer,¹ Ettore Lignelli, Hajime Inoue, Ivana Mižíková,^{2,3} David E. Surate Solaligue,⁴ Heiko Steenbock, Despoina Myti, István Vadász, Susanne Herold, Werner Seeger, Jürgen Brinckmann, and  Rory E. Morty

Department of Lung Development and Remodelling, Max Planck Institute for Heart and Lung Research, member of the German Center for Lung Research (DZL), Bad Nauheim, Germany (T.P., E.L., I.M., D.E.S.S., D.M., W.S., R.E.M.); Department of Internal Medicine (Pulmonology), University of Giessen and Marburg Lung Center (UGMLC), member of the German Center for Lung Research (DZL), Giessen, Germany (T.P., E.L., I.M., D.E.S.S., D.M., I.V., S.H., W.S., R.E.M.); Division of Regenerative Medicine, Department of Plastic and Reconstructive Surgery, St. Marianna University School of Medicine, Kawasaki, Japan (H.I.); and Institute of Virology and Cell Biology (H.S., J.B.) and Department of Dermatology (J.B.), University of Lübeck, Lübeck, Germany,

Received May 29, 2020; accepted September 22, 2020

ABSTRACT

The lysyl hydroxylases (procollagen-lysine 5-dioxygenases) PLOD1, PLOD2, and PLOD3 have been proposed as pathogenic mediators of stunted lung development in bronchopulmonary dysplasia (BPD), a common complication of preterm birth. In affected infants, pulmonary oxygen toxicity stunts lung development. Mice lacking *Plod1* exhibit 15% mortality, and mice lacking *Plod2* or *Plod3* exhibit embryonic lethality. Therefore, to address any pathogenic role of lysyl hydroxylases in stunted lung development associated with BPD, minoxidil was administered to newborn mice in an oxygen toxicity–based BPD animal model. Minoxidil, which has attracted much interest in the management of systemic hypertension and androgenetic alopecia, can also be used to reduce lysyl hydroxylase activity in cultured cells. An in vivo pilot dosing study established 50 mg·kg^{−1}·day^{−1} as the maximum possible minoxidil dose for intraperitoneal administration in newborn mouse pups. When administered at 50 mg·kg^{−1}·day^{−1} to newborn mouse pups, minoxidil was detected in the lungs but did not impact lysine hydroxylation, collagen crosslinking, or lysyl hydroxylase expression in the lungs. Consistent with no impact on mouse lung extracellular matrix

structures, minoxidil administration did not alter the course of normal or stunted lung development in newborn mice. At doses of up to 50 mg·kg^{−1}·day^{−1}, pharmacologically active concentrations of minoxidil were not achieved in neonatal mouse lung tissue; thus, minoxidil cannot be used to attenuate lysyl hydroxylase expression or activity during mouse lung development. These data also highlight the need for new and specific lysyl hydroxylase inhibitors.

SIGNIFICANCE STATEMENT

Extracellular matrix crosslinking is mediated by lysyl hydroxylases, which generate hydroxylated lysyl residues in procollagen peptides. Deregulated collagen crosslinking is a pathogenic component of a spectrum of diseases, and thus, there is interest in validating lysyl hydroxylases as pathogenic mediators of disease and potential “druggable” targets. Minoxidil, administered at the maximum possible dose, did not inhibit lysyl hydroxylation in newborn mouse lungs, suggesting that minoxidil was unlikely to be of use in studies that pharmacologically target lysyl hydroxylation in vivo.

The authors were supported by the Max Planck Society (W.S. and R.E.M.); the German Center for Lung Research [Deutsches Zentrum für Lungenforschung (DZL)] (I.V., S.H., W.S., and R.E.M.), the German Research Foundation [Deutsche Forschungsgemeinschaft (DFG)] through Excellence Cluster EXC2026 [390649896] (I.V., S.H., W.S., and R.E.M.), Collaborative Research Center SFB1213 [268555672] (W.S. and R.E.M.), Clinical Research Unit KFO309 [284237345] (I.V., S.H., W.S., and R.E.M.), and individual research Grants Mo 1789/1-1 [160966624] and Mo 1789/4-1 [420759458] (R.E.M.).

¹Current affiliation: Centre for Paediatric and Adolescent Medicine, Heidelberg University Hospital, Heidelberg, Germany.

²Current affiliation: Regenerative Medicine Program, The Ottawa Hospital Research Institute, Ottawa, Ontario, Canada.

³Current affiliation: Department of Cellular and Molecular Medicine, University of Ottawa, Ottawa, Ontario, Canada.

⁴Current affiliation: Our Lady's Hospital, Navan, Co. Meath, Ireland.
<https://doi.org/10.1124/jpet.120.000138>.

[§] This article has supplemental material available at jpet.aspetjournals.org.

Introduction

The generation of the alveoli, the principal gas-exchange units of the lungs, occurs during the later stages of lung development (Schittny, 2017). The generation of alveoli is stunted in preterm infants that receive oxygen support for respiratory failure at birth because of the deleterious effect of oxygen toxicity on lung development. This culminates in a clinical entity known as bronchopulmonary dysplasia (BPD), leaving affected infants with underdeveloped lungs (Northway et al., 1967). The development of the alveoli relies on the proper deposition and remodeling of the extracellular matrix (ECM) in the immature lung (Jackson et al., 1990; Mariani et al., 1997; Albertine et al., 1999; Mecham, 2018), and perturbations to ECM structures are

ABBREVIATIONS: BPD, bronchopulmonary dysplasia; CE, coefficient of error; CT, cycle threshold; DHLNL, dihydroxylysineonorleucine; ECM, extracellular matrix; HLNL, hydroxylysineonorleucine; HP, hydroxylysylpyridinoline; HPLC, high-performance liquid chromatography; K_{ATP} channel, ATP-sensitive potassium channel; P, postnatal day; PLOD, procollagen-lysine, 2-oxoglutarate 5-dioxygenase.

associated with the stunted lung development seen in patients with BPD (Thibeault et al., 2003; Mizíková and Morty, 2015). Thus, there is interest in identifying the mechanisms of post-translational processing of the ECM during lung development (Lignelli et al., 2019) and, in doing so, identifying enzymatic targets amenable to pharmacological modulation that may form the basis of new clinical management strategies for affected infants.

The inter- and intramolecular crosslinking of collagens, elastin, and other ECM components are key events in the maturation of the ECM. For this reason, families of ECM crosslinking enzymes have received much attention in the context of lung development, including lysyl oxidases (Bland et al., 2007; Kumarasamy et al., 2009), lysyl hydroxylases (Witsch et al., 2014b), and transglutaminases (Witsch et al., 2014a). To this end, a combination of gene ablation and pharmacological intervention studies have highlighted roles for lysyl oxidases (Mizíková et al., 2015) and transglutaminases (Mizíková et al., 2018) in normal lung development and stunted lung development associated with BPD. However, to date, no function for lysyl hydroxylases in normal or aberrant lung development has been validated.

Lysyl hydroxylases, also called procollagen-lysine 5-dioxygenases (EC 1.14.11.4), catalyze the hydroxylation of lysine to hydroxylysine (Kivirikko and Prockop, 1972) in procollagen peptides, which facilitates the formation of collagen crosslinks as well as collagen glycosylation. There are currently three members of the lysyl hydroxylase family: PLOD1, PLOD2, and PLOD3 (Myllylä et al., 2007). Both PLOD1 and PLOD3 catalyze the hydroxylation of lysine residues within the triple helical domain of collagens, whereas PLOD2 catalyzes the hydroxylation of lysine residues in the telopeptides of fibrillar collagens (Gjaltema and Bank, 2017). In addition to lysyl hydroxylase activity, PLOD3 also exhibits hydroxylysyl galactosyltransferase and galactosylhydroxylysyl glucosyltransferase activities (Myllylä et al., 2007). Lysyl hydroxylases have been implicated in a spectrum of clinical pathologies. Lysyl hydroxylase deficiency causes the connective tissue diseases kyphoscoliotic Ehlers-Danlos syndrome (Krane et al., 1972) and Bruck syndrome (Bank et al., 1999). Additionally, lysyl hydroxylases have been proposed to be pathogenic mediators and potentially “druggable” targets in lung disease, including idiopathic pulmonary fibrosis [reviewed in Piersma and Bank (2019)], lung cancer progression (Chen et al., 2015), and the stunted lung development associated with BPD (Witsch et al., 2014b). To provide evidence for a causal role for lysyl hydroxylases in BPD, minoxidil, which is known to reduce lysyl hydroxylase activities in cultured cells, was administered to developing newborn mouse pups in an oxygen toxicity-based experimental animal model of BPD. Our data demonstrate that minoxidil is not suitable for the *in vivo* inhibition of lysyl hydroxylase activity in newborn mice using the intraperitoneal route at 50 mg·kg⁻¹·day⁻¹, which was assessed to be the highest possible dose in newborn mouse pups. These data serve as a cautionary note to investigators about the use of minoxidil in experimental animal models and highlight the need for the identification of new, specific inhibitors of lysyl hydroxylases.

Materials and Methods

Animal Studies. All animal procedures were approved by the local regulatory authority: the Regierungspräsidium Darmstadt

(approval B2/1029, which implements Directive 2010/63/E, the European Union legislation governing the protection of animals used for scientific purposes). Minoxidil, which is reported to reduce lysyl hydroxylase activity in intact cells and tissues (Murad and Pinnell, 1987), both *in vitro* (Zuurmond et al., 2005) and *in vivo* (Eisinger-Mathason et al., 2013), was used in the present study in an attempt to inhibit lysyl hydroxylase function in an experimental animal model of BPD. Newborn C57BL/6J mouse pups (from Charles River, Sülzfeld, Germany) were treated with minoxidil (M4145; Sigma, Taufkirchen, Germany) dissolved in sterile water for injection (A1287301; Thermo-Fisher, Dreieich, Germany). By way of a pilot study, minoxidil was administered at doses of 5 and 50 mg·kg⁻¹·day⁻¹ via the intraperitoneal route starting on the day of birth, designated postnatal day (P)1, and daily administration was continued up to and including P13. Mice were killed with sodium pentobarbital (Narcoren, 500 mg·kg⁻¹, intraperitoneal; Bohringer Ingelheim, Germany) on P14. For studies on the impact of minoxidil administration on collagen crosslinking and the development of the alveolar architecture, mouse pups treated either with water for injection (daily, in a volume of 10 μ l·g⁻¹; as a control) or with minoxidil (50 mg·kg⁻¹·day⁻¹; in a volume of 10 μ l·g⁻¹) were exposed to normoxic (21% O₂) or hyperoxic (85% O₂) conditions in an A-Chamber (Biospherix, Parish, NY) in a well established experimental animal model of BPD (Alejandre-Alcázar et al., 2007; Nardiello et al., 2017). Nursing dams were rotated every 24 hours between normoxia- and hyperoxia-exposed litters to minimize the toxic effects of 85% O₂ exposure on adult mice. Dams and pups were maintained on a 12-hour light/dark cycle and received food (Altromin 1314 standard diet for rodents; Altromin Spezialfutter GmbH, Lage, Germany) and tap water *ad libitum*.

Cell Culture and Cell Treatments. NIH/3T3 cells (ATCC CRL-1658; American Type Culture Collection, Manassas, VA) were employed as an *in vitro* model of mouse fibroblasts (Todaro and Green, 1963) and were passaged as per the manufacturer's recommendations. For studies on minoxidil and minoxidil sulfate, cells were treated with either vehicle (water for injection), minoxidil (0.1 or 1.0 mM), or minoxidil sulfate (M7920; 0.1 or 1.0 mM; Sigma-Aldrich, Dreieich, Germany) for 48 hours. RNA was extracted from cultured cells using a protocol described previously (Ruiz-Camp et al., 2019), and *Plod1*, *Plod2*, and *Plod3* steady-state mRNA abundance was assessed by real-time reverse transcription polymerase chain reaction (RT-PCR) as described below. For studies with modulators of sulfotransferase activity, cells were treated with vehicle (water for injection), sodium chlorate (403016; 50 mM; Sigma-Aldrich), acetaminophen (A7085; 5 mM; Sigma-Aldrich), or 2,4-dichloro-6-nitrophenol (225436; 1 μ M; Merck, Darmstadt, Germany) for 1 hour, after which prewarmed medium was replaced with media containing minoxidil (to 1 mM) as well as the corresponding modulator. Cells were incubated for 48 hours, and *Plod1*, *Plod2*, and *Plod3* steady-state mRNA abundance was assessed by real-time RT-PCR as described below.

HPLC Determination of Minoxidil. Lung tissue samples were homogenized in 0.4 M HClO₄ (0.5 ml) using a Polytron Homogenizer (Thomas Scientific, Swedesboro, NJ). Homogenates were clarified first by centrifugation at 14,500g (15 minutes, 4°C), and the supernatant was passed through a 0.22- μ m filter prior to application to a Kaseisorb octadecyl-silica (4.6 \times 150 mm, 5 μ m) HPLC column. The HPLC column was integrated into a Jasco Systems 4000 HPLC system (Jasco System Co., Tokyo, Japan) with a PU-4180 pump, an AS-4050 autosampler, a UV-4075 detector, and a CO-2067 column oven. Sample components were eluted with 0.1 M HCOOH/methanol, 65:35, pH 2.0, at a flow-rate of 1.0 ml/min at 40°C, and eluates were detected at an absorbance of 240 nm (Ichida et al., 2020). For initial range finding, homogenates prepared from untreated lungs were spiked with minoxidil (Fig. 1A).

Polymerase Chain Reaction Analysis To Determine Sex Genotype and mRNA Expression. Sex genotyping of mouse pups was undertaken essentially as described in Lambert et al. (2000), in which the *Sry* and *Il3* loci were employed to discriminate between male and female sex using the protocol described by the authors

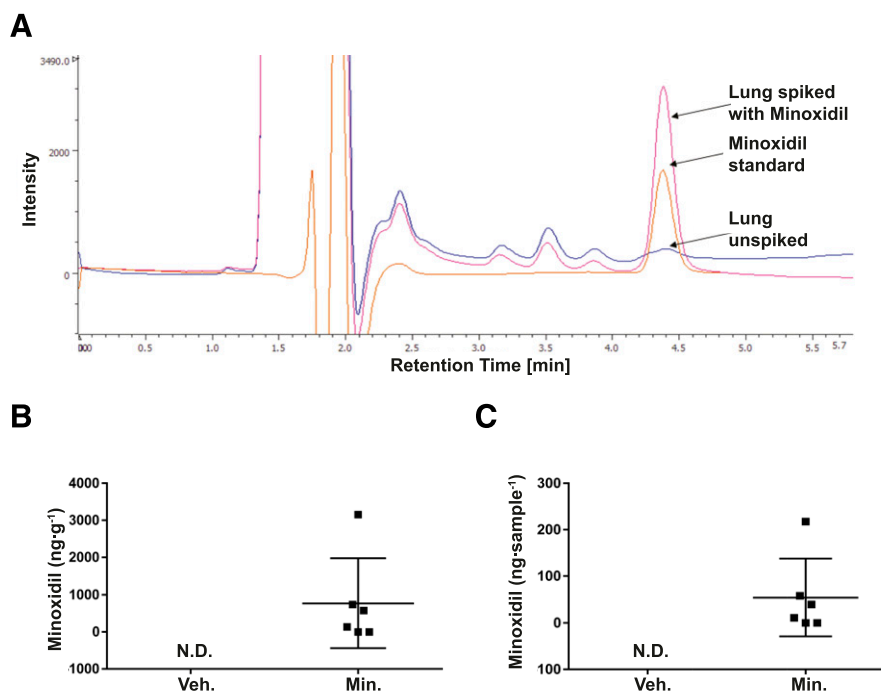


Fig. 1. Quantification of minoxidil in the developing mouse lung. (A) Representative original HPLC trace illustrating the identification of minoxidil, either spiked in perchloric acid–extracted lung tissue or as a minoxidil standard, in which the background trace for unspiked lung extracts is also depicted. Quantitative determinations of minoxidil in extracts prepared from the lungs of developing mouse pups ($n = 6$ mouse pups per group) treated either with vehicle (Veh., water for injection) or minoxidil (Min., 50 $\text{mg}\cdot\text{kg}^{-1}\cdot\text{day}^{-1}$) are presented as (B) minoxidil ($\text{ng}\cdot\text{g}^{-1}$) and (C) minoxidil ($\text{ng}\cdot\text{lung sample}^{-1}$). N.D., not detected.

previously (Nardiello et al., 2017). The primers employed are listed in Table 1.

RNA samples were prepared from mouse lungs, testes, gut, and liver as described previously (Mizíková et al., 2015, 2017). Steady-state mRNA transcript levels were assessed by real-time RT-PCR employing the primers listed in Table 1, which amplified the mRNA transcripts encoding the three known mouse lysyl hydroxylases (designated *Plod1*, *Plod2*, and *Plod3*), using the *Polr2a* mRNA transcript as a reference gene. Additionally, the steady-state abundance of mRNA transcripts encoding sulfotransferases that are known to convert minoxidil to minoxidil sulfate (*Sult1a1*, *Sult1b1*, *Sult1c1*, *Sult1c2*, *Sult2a1*, *Sult1d1*, and *Sult1e1*) as well as the subunits of a minoxidil target—the ATP-sensitive potassium channel (K_{ATP} channel), *Abcc8*, *Abcc9*, *Kcnj8*, and *Kcnj1*—were also profiled by real-time RT-PCR.

Real-time RT-PCR amplification and analysis were performed using the protocols described previously (Mizíková et al., 2015, 2017). Real-time RT-PCR data are presented as the difference in cycle threshold (CT), denoted ΔCT , which reflects the relationship $\text{CT}(\text{Polr2a}) - \text{CT}(\text{gene of interest})$. The fold-change in mRNA abundance was determined from the following relationship: $\text{fold-change} = 2^{|\Delta\Delta\text{CT}|}$.

Immunoblotting. Steady-state protein expression levels of PLOD1 were assessed in protein extracts prepared from the lungs of mouse pups exposed either to normoxic (21% O_2) or hyperoxic (85% O_2) conditions for the first 14 days of postnatal life, as well as in adult (3-month-old) mouse lungs. Protein extracts were resolved on a 12.5% reducing SDS-PAGE gel and electroblotted onto a nitrocellulose membrane. PLOD1 was detected with a rabbit anti-mouse PLOD1 antibody (12475-1-AP; 1:1000; Proteintech, Manchester, UK). Loading equivalence was verified by reprobing the same nitrocellulose membrane for β -actin using a rabbit anti-human β -actin antibody (4967; 1:2000; Cell Signaling Technology, Frankfurt am Main, Germany). Immune complexes were detected with a goat anti-rabbit IgG horseradish peroxidase conjugate (31460; 1:3000; ThermoFisher Scientific, Waltham, MA). The pixel density of immunoblot bands was determined by densitometry, and the pixel density of the PLOD1 band was related to the pixel density of the corresponding β -actin band in the same lane using Fiji software (Schindelin et al., 2012).

Assessment of Collagen Protein and Crosslinks. The abundance of insoluble collagen and elastin in mouse lungs, as well as the abundance of hydroxylysine—the enzymatic product of lysyl

hydroxylases—and the abundance of the collagen crosslinks dihydroxyisynonorleucine (DHLNL), hydroxylsypiridinoline (HP), and hydroxyisynonorleucine (HLNL), was determined using the protocol previously described by the authors (Brinckmann et al., 2005; Nave et al., 2014; Mizíková et al., 2015, 2018). The collagen crosslink nomenclature employed in the present study refers to the reduced variants of the intermediate collagen crosslinks DHLNL and HLNL.

Design-Based Stereology for the Analysis of Lung Architecture. Design-based stereology serves as the gold standard for the quantitative assessment of the lung architecture, following the American Thoracic Society/European Respiratory Society recommendations for quantitative assessment of lung structure (Hsia et al., 2010). The stereological approach employed in the present study was described by the authors in detail previously (Mizíková et al., 2015, 2018). Mouse lungs were fixed by intratracheal instillation of 1.5% (m/v) paraformaldehyde and 1.5% (m/v) glutaraldehyde in 150 mM HEPES, pH 7.4, for 24 hours at 4°C, in which fixative was instilled into lungs at a hydrostatic pressure of 20 cmH_2O . The total lung volume was assessed using Cavalieri's principle. Agar-embedded mouse lungs were cut into 3-mm slabs, which were treated with sodium cacodylate, osmium tetroxide, and uranyl acetate and were then embedded in glycol methacrylate (Technovit 7100, catalog number 64709003; Heraeus Kulzer, Hanau, Germany). These Technovit blocks were then sectioned at 2- μm intervals and were stained with Richardson's stain. All slides were scanned using a NanoZoomer-XR C12000 Digital slide scanner (Hamamatsu). For the estimation of the alveolar density and total number of alveoli in the mouse lungs, every first and third section of a consecutive series of sections was assessed. For all other parameters (mean linear intercept, the arithmetic mean septal thickness, gas-exchange surface area, and gas-exchange surface density), every 10th section was assessed. Analyses were made using the Visiopharm NewCast computer-assisted stereology system (VIS 4.5.3).

Statistics and Stereological Precision. Data are presented as means \pm S.D. Differences between groups were assessed by one-way ANOVA with Tukey's post hoc test for multiple comparisons, whereas two-group comparisons were performed with an unpaired Student's *t* test. *P* values <0.05 were regarded as significant. All statistical analyses were performed with GraphPad Prism 6.0. The presence of

TABLE 1

Primers employed for polymerase chain reaction analysis

Gene	Primer	Primer sequence, 5'–3'
<i>Abcc8</i>	Forward	TGAGCATTGGAAGACCCTCAT
	Reverse	CAGCACCGAAGATAAGTTGTCA
<i>Abcc9</i>	Forward	CACACCGAGTGAATCAAAA
	Reverse	ATCCATTGTACCTTTATGGCA
<i>Il3</i>	Forward	GGGACTCCAAGCTTCAATCA
	Reverse	TGGAGGAGGAAGAAAAGCAA
<i>Kcnj8</i>	Forward	AAGAGCATCATCCCGAGGA
	Reverse	ATGTTCTTGTGTGCCAGGTTG
<i>Kcnj11</i>	Forward	AAGGGCATATCCCTGAGGAA
	Reverse	TTGCCTTTCTTGGACACGAAG
<i>Plod1</i>	Forward	GAAGGATGACGCCAAGCTAGA
	Reverse	TGAAGAACTGAGCTGAACGCT
<i>Plod2</i>	Forward	GAGAGGCGGTGATGGAATGAA
	Reverse	ACTCGGTAAACAAGATGACCAGA
<i>Plod3</i>	Forward	ATGTGGCTCGAACAGTTGGTG
	Reverse	TTGCCAGAATCACGTCGTAGC
<i>Polr2a</i>	Forward	CTAAGGGGCGAGCCAAAGAAAC
	Reverse	CCATTGAGCATACAACCTCTAGGC
<i>Sry</i>	Forward	TGGGACTGGTGACAATTGTC
	Reverse	GAGTACAGGTGTGCAGCTCT
<i>Sult1a1</i>	Forward	AACATGGAGCCCTTGCCTAAA
	Reverse	ATGAGCACATCATCAGGCCAG
<i>Sult1b1</i>	Forward	GCACACCAGGTGACATTGTAA
	Reverse	CCGAGGTGATGGAGTTTCTTTC
<i>Sult1c1</i>	Forward	AACATGCAGCCAGAAACCAG
	Reverse	CGGGCTTTGCTTGGAAAGTTC
<i>Sult1c2</i>	Forward	ATGGCCTTGACCCAGAAC
	Reverse	CTTGGCCTCGAAGGTCTGAAT
<i>Sult2a1</i>	Forward	GGTTTGAGCATGTTCTGTGGC
	Reverse	TGGCTTGGAAGAGCTGTACT
<i>Sult1d1</i>	Forward	TCTTCAGGAGGGAGTTAGTGG
	Reverse	GGCCGGGCTTCAAATGACT
<i>Sult1e1</i>	Forward	ATGGAGACTTCTATGCCTGAGT
	Reverse	ACACAACTTCACTAATCCAGGTG
<i>Sult3a1</i>	Forward	TATTTTGAGGGTTCATCGAACAG
	Reverse	GGTGATGGCATTTTGGCATAGT
<i>Sult5a1</i>	Forward	ATGACTGAGCGCATGAACACC
	Reverse	CCACAAGTGACCCTCACAGA

statistical outliers was tested by Grubbs' test, and if found, statistical outliers were removed. If an outlier within a group was removed, the data from that animal were removed from all groups. The coefficient of error (*CE*), the *CV*, and the squared ratio between both (CE^2/CV^2) were calculated for each stereological parameter, in which a $CE^2/CV^2 < 0.5$ validated the precision of the measurements.

Results

Hyperoxia Affected Lysyl Hydroxylase mRNA and Protein Steady-State Levels. Exposure of newborn mouse pups to 85% O_2 for the first 14 days of postnatal life increased steady-state mRNA levels of *Plod1* but not of *Plod2*, and steady-state levels of *Plod3* mRNA were decreased in 85% O_2 -exposed lungs (Fig. 2). The increase in *PLOD1* protein expression was validated by immunoblot (Fig. 3A, quantified in Fig. 3B; full uncropped immunoblots are provided in Supplemental Fig. 1). In pilot studies, minoxidil administered daily at doses of 5 and 50 $mg \cdot kg^{-1} \cdot day^{-1}$ via the intraperitoneal route was well tolerated by mouse newborns and neonates. The administration of higher doses of minoxidil was not possible, because of a combination of stock solution solubility limit and the maximum injectable volume in newborn and neonatal mice. Increasing the minoxidil stock solution concentration from 5.0 to 7.5 $mg \cdot ml^{-1}$ resulted in only partial solubility in water for injection, which was also observed using 10% (v/v) ethanol and 10% (v/v) DMSO (Supplemental Video 1). For this reason, all subsequent data were obtained using

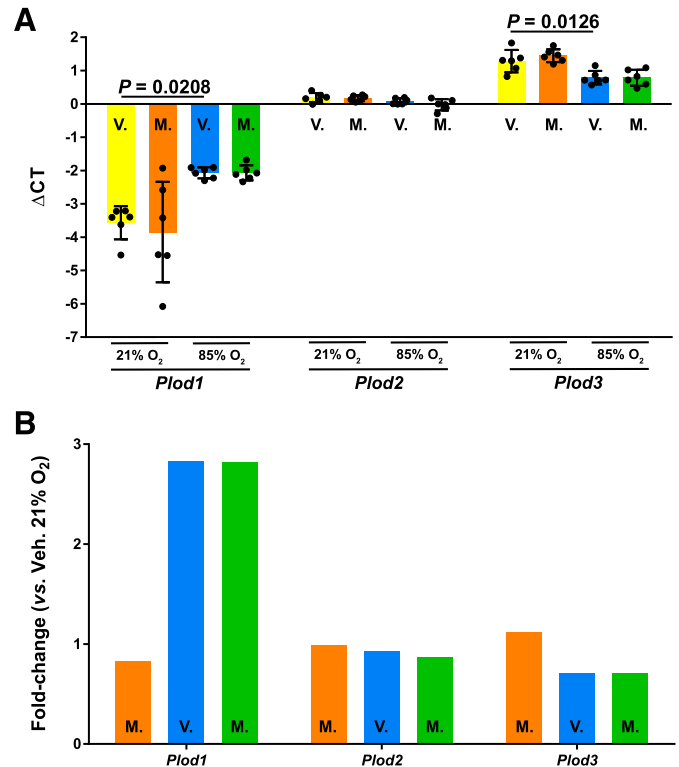


Fig. 2. Assessment of steady-state levels of lysyl hydroxylase mRNA transcripts in the lungs of mouse pups. (A) The steady-state mRNA levels for *Plod1*, *Plod2*, and *Plod3* were assessed by real-time RT-PCR in total RNA pools isolated from the lungs of mouse pups at postnatal day 14 that had been exposed to 21% O_2 (warm colors: yellow and orange) or 85% O_2 (cool colors: blue and green) for the first 2 weeks of postnatal life, with concomitant treatment with water for injection as solvent vehicle (V., yellow or blue bars) or minoxidil dissolved in water for injection (M., orange or green). Data reflect mean $\Delta CT \pm S.D.$ ($n = 6$ animals per experimental group, in which each data point represents an experimental animal). *P* values comparing all four data sets were assessed by one-way ANOVA with Tukey's post hoc test. Three sets of statistical comparisons are presented: one set that compares the two vehicle-treated groups (21% O_2 vs. 85% O_2), and two additional sets, each comparing the impact of minoxidil (vehicle-treated vs. minoxidil-treated) under 21% O_2 or under 85% O_2 conditions. Only the statistical comparisons in which $P < 0.05$ are presented. (B) Data in (A) were transformed to fold-change values, which are described relative to the vehicle-treated 21% O_2 -exposed group, the minoxidil-treated 21% O_2 -exposed group (orange), vehicle-treated 85% O_2 -exposed group (blue bar), and minoxidil-treated 85% O_2 -exposed group (green).

a minoxidil dose of 50 $mg \cdot kg^{-1} \cdot day^{-1}$, representing the maximum possible dose.

Minoxidil Administration at 50 $mg \cdot kg^{-1} \cdot day^{-1}$ Yielded Detectable Minoxidil Levels in Developing Mouse Lungs. Minoxidil could be detected in perchloric acid-extracted lung tissue (Fig. 1A). Using a minoxidil dosing regimen of 50 $mg \cdot kg^{-1} \cdot day^{-1}$, minoxidil was detected in mouse lungs harvested at P14 at concentrations of approximately 0–3000 $ng \cdot g^{-1}$ wet lung tissue (Fig. 1B) or 0–200 $ng \cdot sample^{-1}$ (Fig. 1C).

Hyperoxia Affected Cytosolic Sulfotransferase and K_{ATP} Channel Subunit mRNA Steady-State Levels. Although the mechanism of action of minoxidil on lysyl hydroxylase gene expression is not known, it is known that minoxidil must be converted to minoxidil sulfate by cytosolic sulfotransferases (EC 2.8.2.-) to stimulate hair follicles when minoxidil is used to manage androgenetic alopecia (Buhl et al., 1990). The expression of selected sulfotransferases (Alnouti and Klaassen,

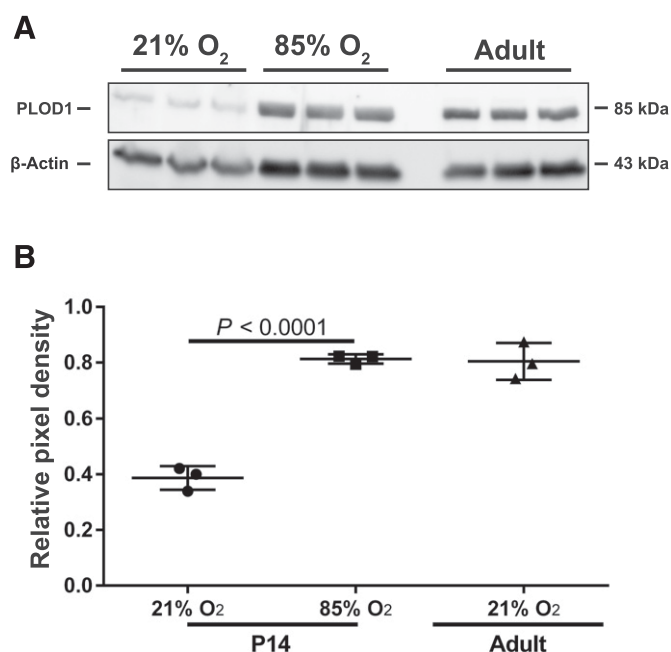


Fig. 3. Assessment of steady-state levels of PLOD1 protein abundance in the lungs of mouse pups. (A) Immunoblot of PLOD1 in protein extracts from the lungs of mouse pups exposed to 21% O₂ or 85% O₂ for the first 14 days of postnatal life (P14) or adult mice (exposed to 21% O₂). β-Actin served as a control for loading equivalence. (B) Densitometric comparison of the pixel density of the PLOD1 bands in (A) to the pixel density of the β-actin bands in (A). Data reflect mean relative pixel density ± S.D. ($n = 3$ mice per group). Data sets were compared using a one-way ANOVA with a Tukey's post hoc test. The full uncropped immunoblot from (A) is provided in Supplemental Fig. 1.

2006) was detected in the developing mouse lungs, and mRNA transcript abundance was affected by hyperoxia exposure: *Sult1c1*, *Sult1c2*, and *Sult3a1* mRNA transcripts exhibited reduced abundance, whereas *Sult1d1* and *Sult5a1* exhibited increased mRNA transcript abundance in the lungs of hyperoxia-exposed mouse pups, and *Sult1a1* mRNA transcript levels were unchanged (Supplemental Fig. 2A). *Sult1b1*, *Sult1e1*, and *Sult2a1* mRNA transcripts were not detected in the lungs (Supplemental Fig. 2B); however, they could be detected in the present study in the mouse liver, gut, or testis, which is in line with an earlier mouse organ profiling report (Alnouti and Klaassen, 2006).

The mechanism of minoxidil action in hair follicles is thought to be mediated by opening K_{ATP} channels (Messenger and Rundegren, 2004). Thus, the expression of K_{ATP} channel subunits was profiled in neonate and adult mouse lung tissue. The pore-forming subunits of the K_{ATP} channels (*Kcnj8* and *Kcnj11*) exhibited increased steady-state mRNA transcript levels in adult mouse lungs versus neonate mouse lungs, whereas the sulfonylurea receptor subunits (*Abcc8* and *Abcc9*) exhibited decreased steady-state mRNA transcript levels in adult mouse lungs versus neonate mouse lungs (Supplemental Fig. 3). In neonate mouse lungs, hyperoxia exposure was without effect on the expression of *Kcnj8*, *Kcnj11*, or *Abcc8*; however, the mRNA transcript abundance of *Abcc9* was increased (Supplemental Fig. 3). Thus, both age and oxygen toxicity can affect the steady-state mRNA abundance of both cytosolic sulfotransferases and of K_{ATP} channel subunits in mouse lungs.

Minoxidil Sulfate Is More Potent than Minoxidil at Reducing Lysyl Hydroxylase mRNA Transcript Abundance. In cell culture studies in NIH/3T3 cells, minoxidil sulfate at 1 mM was more potent at reducing the steady-state mRNA transcript abundance of *Plod1*, *Plod2*, and *Plod3* than was minoxidil. This effect was not observed at concentrations of 0.1 mM comparing both compounds (Supplemental Fig. 4). These data suggest that sulfation of minoxidil can enhance the ability of minoxidil to reduce steady-state mRNA abundance of lysyl hydroxylase mRNA transcripts.

Modulators of Sulfotransferase Activity Affect the Capacity of Minoxidil To Reduce Lysyl Hydroxylase mRNA Transcript Abundance. The conversion of minoxidil to minoxidil sulfate is undertaken by a sequence of enzymatic reactions: sulfate adenylyltransferase (EC 2.7.7.4) is the first enzyme in the synthesis of 3'-phosphoadenosine 5'-phosphosulfate, which donates sulfate to minoxidil, and is inhibited by chlorate (Baeuerle and Huttner, 1986). Sulfotransferases (EC 2.8.2.-) catalyze the transfer of a sulfate group from 3'-phosphoadenosine 5'-phosphosulfate to an acceptor alcohol and can be inhibited with 2,4-dichloro-6-nitrophenol (Rein et al., 1982). Additionally, acetaminophen, which is a sulfate scavenger, may be used to prevent the incorporation of sulfate into minoxidil (Reiter and Weinshilboum, 1982). Both chlorate and 2,4-dichloro-6-nitrophenol attenuated the ability of minoxidil to reduce steady-state mRNA transcript abundance of *Plod1* and *Plod3* (Supplemental Fig. 5). These data support the idea that sulfation of minoxidil enhances the ability of minoxidil to reduce steady-state mRNA abundance of lysyl hydroxylase mRNA transcripts.

Minoxidil Administration Did Not Affect Lysine Hydroxylation in Developing Mouse Lungs. During normal lung development, under conditions of 21% O₂, daily administration of 50 mg·kg⁻¹·day⁻¹ minoxidil to mouse pups over the first 14 days of postnatal life had no effect on the abundance of hydroxylysine in the lung (Fig. 4A). Similarly, total collagen per unit protein was unchanged by minoxidil treatment (Fig. 4B). Minoxidil treatment did reduce the abundance of elastin in total protein by ~7%, from 14% ± 0.28% to 13% ± 0.71% (Fig. 4C), although the collagen/elastin ratio remained unchanged (Fig. 4D). Under conditions of 85% O₂, in which postnatal lung development is stunted, the abundance of hydroxylated lysine residues was increased compared with 21% O₂ conditions (Fig. 4A); however, minoxidil administration did not impact hydroxylysine abundance comparing vehicle-treated mice versus minoxidil-treated mice (both under 85% O₂ conditions) (Fig. 4A). Exposure of mouse pups to 85% O₂ increased total collagen in the lung (Fig. 4B), decreased total elastin in the lung (Fig. 4C), and increased the collagen/elastin ratio in the lung (Fig. 4D). Minoxidil treatment did not attenuate the effect of 85% O₂ exposure on total collagen, elastin, and the collagen/elastin ratio in the lung. Thus, these data indicate that parenteral administration of minoxidil did not reduce the abundance of lysine hydroxylation, suggesting that lysyl hydroxylases were comparably active in the lungs of vehicle-treated and minoxidil-treated mouse lungs.

Minoxidil Administration Was Largely without Impact on Immature Bifunctional and Mature Trifunctional Collagen Crosslinks Containing Hydroxylysine. Exposure of developing mouse lungs to 85% O₂ over the first 14 days of postnatal life consistently affected the abundance of collagen

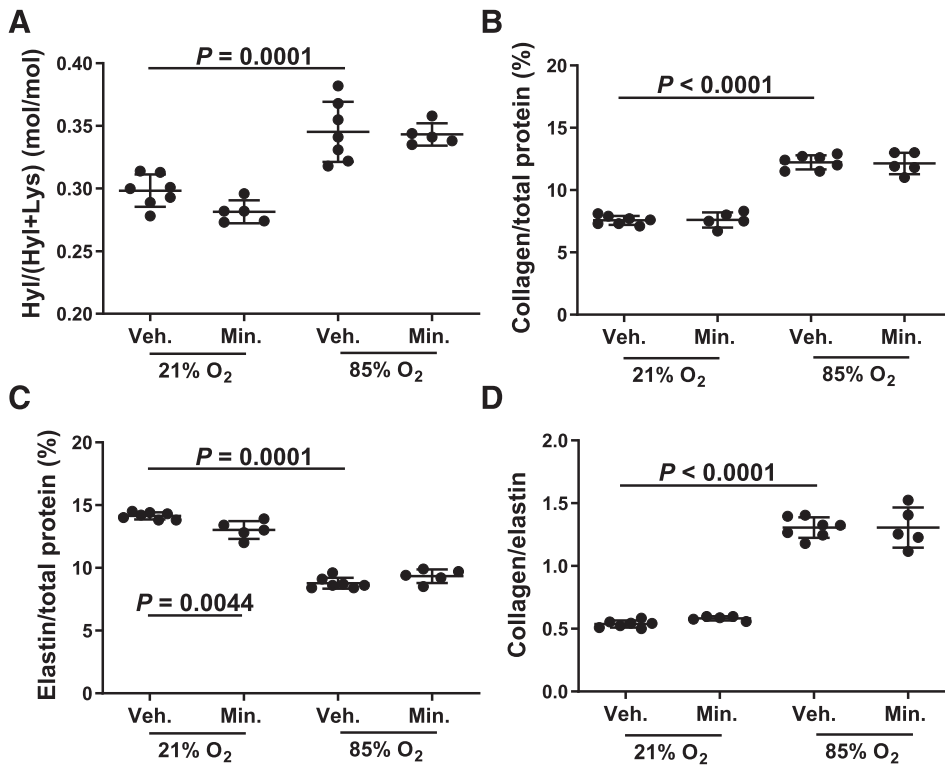


Fig. 4. Abundance of hydroxylysine (Hyl), collagen, and elastin in developing mouse lungs. The abundance of (A) hydroxylysine, (B) collagen, (C) elastin, and (D) the collagen/elastin ratio were determined for the lungs of developing wild-type C57BL/6J mouse pups exposed to either 21% O₂ or 85% O₂ for the first 14 days of postnatal life with concomitant daily administration of solvent vehicle (Veh.) or minoxidil (Min.). Data reflect means \pm S.D. ($n = 5-7$ experimental animals per group; each data point represents an experimental animal). Data sets were compared by one-way ANOVA with Tukey's post hoc test. Three sets of statistical comparisons are presented: one set that compares the two vehicle-treated groups (21% O₂ vs. 85% O₂), and two additional sets, each comparing the impact of minoxidil (vehicle-treated vs. minoxidil-treated) under 21% O₂ or under 85% O₂ conditions. Only the statistical comparisons in which $P < 0.05$ are presented. Lys, lysine.

crosslinks. Exposure of mouse pups to 85% O₂ increased the abundance of the mature trifunctional HP collagen crosslink (Fig. 5A), as well as the abundance of the immature bifunctional DHLNL collagen crosslink (Fig. 5B). In contrast, 85% O₂ exposure decreased the abundance of the alternative immature bifunctional HLNL collagen crosslink (Fig. 5C), leading to an increase in the DHLNL/HLNL ratio in 85% O₂-exposed lungs compared with 21% O₂-exposed mouse lungs (Fig. 5D). Minoxidil did not impact the abundance of collagen crosslinks comparing vehicle versus minoxidil treatments within the normoxia- or hyperoxia-exposed mouse groups (Fig. 5), with the single exception of DHLNL in the normoxia-exposed mouse group (Fig. 5D). Thus, minoxidil treatment was without effect on the abundance of hydroxylysine-containing collagen crosslinks within the hyperoxia-exposed mouse groups.

Minoxidil Administration Was without Impact on Postnatal Lung Development. Exposure of newborn mice to 85% O₂ for the first 14 days of postnatal life appreciably stunted the development of the lung architecture, as was evident by visual inspection of lung sections from vehicle-treated, 21% O₂-exposed mouse pups (Fig. 6A) compared with vehicle-treated, 85% O₂-exposed mouse pups (Fig. 6B). Quantitative assessment of lung structure using design-based stereology supported this observation (Table 2), in which a decreased density of the gas-exchange surface area (Fig. 6E) and a decreased gas-exchange surface area (Fig. 6F) were noted, along with an increased septal thickness (Fig. 6G) and mean linear intercept (Fig. 6H). In line with a reduced gas-exchange surface area, both a decreased alveolar density (Fig. 6I) and a consequently reduced total number of alveoli in the lung (Fig. 6J) were also noted. Visual inspection of lung sections prepared from mice treated with minoxidil (Fig. 6, C and D) did not suggest any impact of minoxidil treatment on normal (under 21% O₂) or stunted (under 85% O₂) lung

development. Consistent with this observation, no impact of minoxidil treatment on any of the stereological parameters that describe the lung architecture was noted (Fig. 6, E–J; Table 2). Thus, minoxidil treatment did not alter the course of normal lung development or that of stunted lung development associated with oxygen toxicity.

Discussion

The mechanisms of normal and stunted lung development associated with BPD include a pivotal role for the ECM (Mizíková and Morty, 2015; Zhou et al., 2018). Correct spatiotemporal generation of elastin fibers is essential for lung development (Branchfield et al., 2016), and disordered elastin (Mariani et al., 1997; Mecham, 2018) and collagen (Thibeault et al., 2003) deposition is a hallmark of stunted lung development. Post-translational ECM modification and remodeling is in part directed by intra- and intermolecular crosslinks formed by the lysyl oxidase, lysyl hydroxylase, and transglutaminase crosslinking enzymes (Mecham, 2012). This has stimulated interest in targeting crosslinking enzymes in lung development. Pharmacological interventions that prevent or reverse stunted lung development by modulating crosslink formation may also form the basis of novel strategies to manage the pulmonary consequences of preterm birth. Studies addressing the roles and therapeutic targeting of lysyl oxidases (Mizíková et al., 2015) and transglutaminases (Mizíková et al., 2018) in animal models of BPD have already been initiated.

Although lysyl hydroxylase expression is deregulated by oxygen toxicity (Witsch et al., 2014b) and is associated with BPD (Witsch et al., 2014b), no studies to date have addressed causal roles for lysyl hydroxylases in BPD. Lysyl hydroxylases

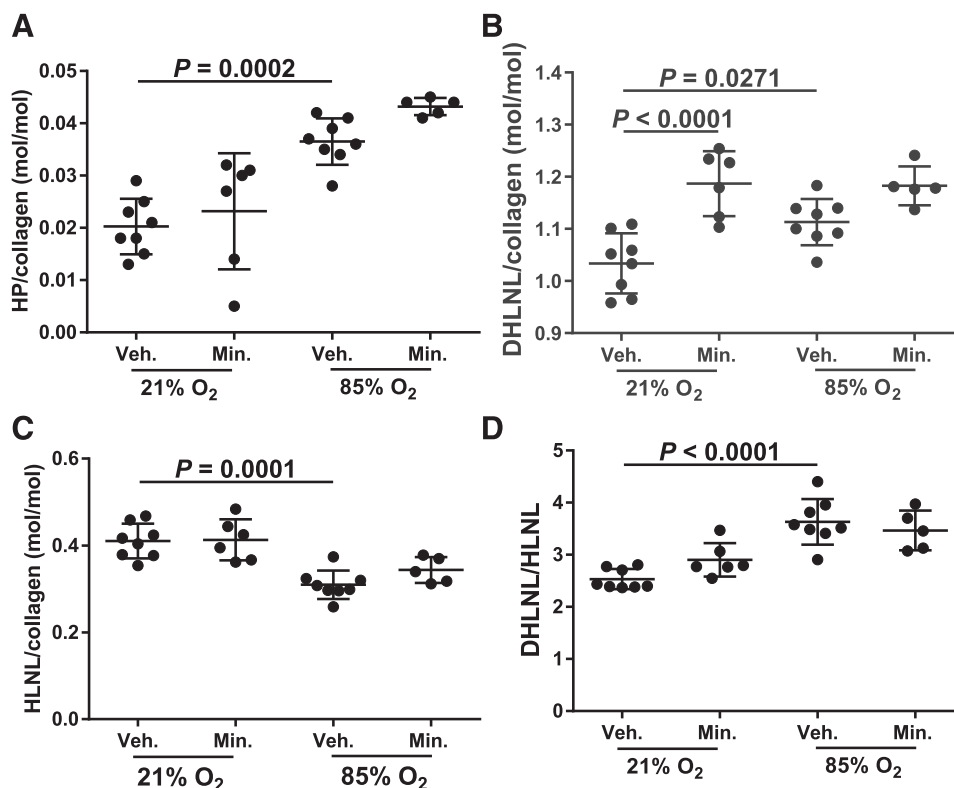


Fig. 5. Abundance of collagen crosslinks in developing mouse lungs. The abundance of (A) HP per unit collagen, (B) DHLNL per unit collagen, (C) HLNL per unit collagen, and (D) the DHLNL/HLNL ratio were determined for the lungs of developing wild-type C57BL/6J mouse pups exposed to either 21% O₂ or 85% O₂ for the first 14 days of postnatal life with concomitant daily administration of solvent vehicle (Veh.) or minoxidil (Min.). Data reflect means \pm S.D. ($n = 5$ –8 experimental animals per group; each data point represents an experimental animal). Data sets were compared by one-way ANOVA with Tukey's post hoc test. Three sets of statistical comparisons are presented: one set that compares the two vehicle-treated groups (21% O₂ vs. 85% O₂), and two additional sets, each comparing the impact of minoxidil (vehicle-treated vs. minoxidil-treated) under 21% O₂ or under 85% O₂ conditions. Only the statistical comparisons in which $P < 0.05$ are presented.

generate hydroxylysine, first described by Van Slyke and Hiller (1921), through hydroxylation of lysyl residues in procollagen. The lysyl hydroxylase family contains three procollagen-lysine 5-dioxygenases: PLOD1, PLOD2, and PLOD3 (Myllylä et al., 2007). *Plod1*^{−/−} mice are largely viable (a 15% mortality rate due to aortic rupture is reported) (Takaluoma et al., 2007); but *Plod2*^{−/−} (Kasamatsu et al., 2019) and *Plod3*^{−/−} (Ruotsalainen et al., 2006) mice exhibit embryonic lethality, in which less hydroxylysine and aberrant collagen structures are reported in *Plod1*^{−/−} and *Plod3*^{−/−} mouse lungs. The lethality of *Plod* gene deletions in mice demands pharmacological interventions to explore the role—and targeting potential—of lysyl hydroxylases in stunted lung development.

No specific inhibitors of lysyl hydroxylases exist. Minoxidil was initially developed as an antihypertensive (Zins, 1988) because of its vasodilator activity (Gottlieb et al., 1972); but the utility of systemic minoxidil is limited as a result of edema provoked by minoxidil (Zins, 1988). The baldness reversal observed in a patient receiving minoxidil for hypertension (Zappacosta, 1980) led to widespread use of topical minoxidil (Rogaine) to reverse androgenetic alopecia (Zins, 1988), possibly through potassium channel-opening properties of minoxidil (Messenger and Rundegren, 2004). Subsequent in vitro studies in skin fibroblasts revealed that minoxidil inhibited lysyl hydroxylases (Murad et al., 1992) but not prolyl hydroxylases (Cardinale and Udenfriend, 1974), which was attributed to the inhibition of *Plod1*, *Plod2*, and *Plod3* gene transcription (Murad and Pinnell, 1987; Pinnell and Murad, 1987; Hautala et al., 1992; Murad et al., 1992; Zuurmond et al., 2005) and possibly direct competitive enzyme inhibition (Shao et al., 2018). These in vitro studies suggested the possibility of using minoxidil to target lysyl hydroxylases in vivo.

Increased lung lysyl hydroxylase protein and mRNA abundance has been reported in a hyperoxia-based experimental BPD model in mice (Witsch et al., 2014b). Those observations were confirmed in the present study. Minoxidil was then administered in the experimental BPD mouse model in an effort to blunt pathologically increased lysyl hydroxylase expression and activity. Intraperitoneal administration of minoxidil to newborn mouse pups was well tolerated at 5 and 50 mg·kg^{−1}·day^{−1}, without evidence of hypertrichosis or other obvious side-effects by P14. Although minoxidil reduced *Plod1*, *Plod2*, and *Plod3* expression in cell culture (Murad and Pinnell, 1987; Pinnell and Murad, 1987; Hautala et al., 1992; Murad et al., 1992; Zuurmond et al., 2005), minoxidil administration did not impact steady-state *Plod1*, *Plod2*, and *Plod3* mRNA transcript levels in the lungs of minoxidil-treated mice. In line with sustained expression of *Plod1*, *Plod2*, and *Plod3* despite minoxidil treatment, no reduction in lung hydroxylysine abundance or attenuation of hyperoxia-driven perturbations to hydroxylysine-based crosslinks or lung development were noted.

Data are also presented that indicate that minoxidil sulfate is more potent than minoxidil at reducing lysyl hydroxylase mRNA transcript abundance. This is consistent with minoxidil sulfate being the active minoxidil metabolite that stimulates hair follicles in androgenetic alopecia. Thus, the authors considered whether the conversion of minoxidil to minoxidil sulfate by cytosolic sulfotransferases may be blunted in hyperoxia-exposed lungs, given that hyperoxia affected the ability of minoxidil to modulate total elastin levels (Fig. 4C) and DHLNL abundance in collagen (Fig. 5B). Indeed, by profiling all cytosolic sulfotransferases that are known to metabolize minoxidil to minoxidil sulfate (Allali-Hassani et al., 2007), it was evident that hyperoxia exposure

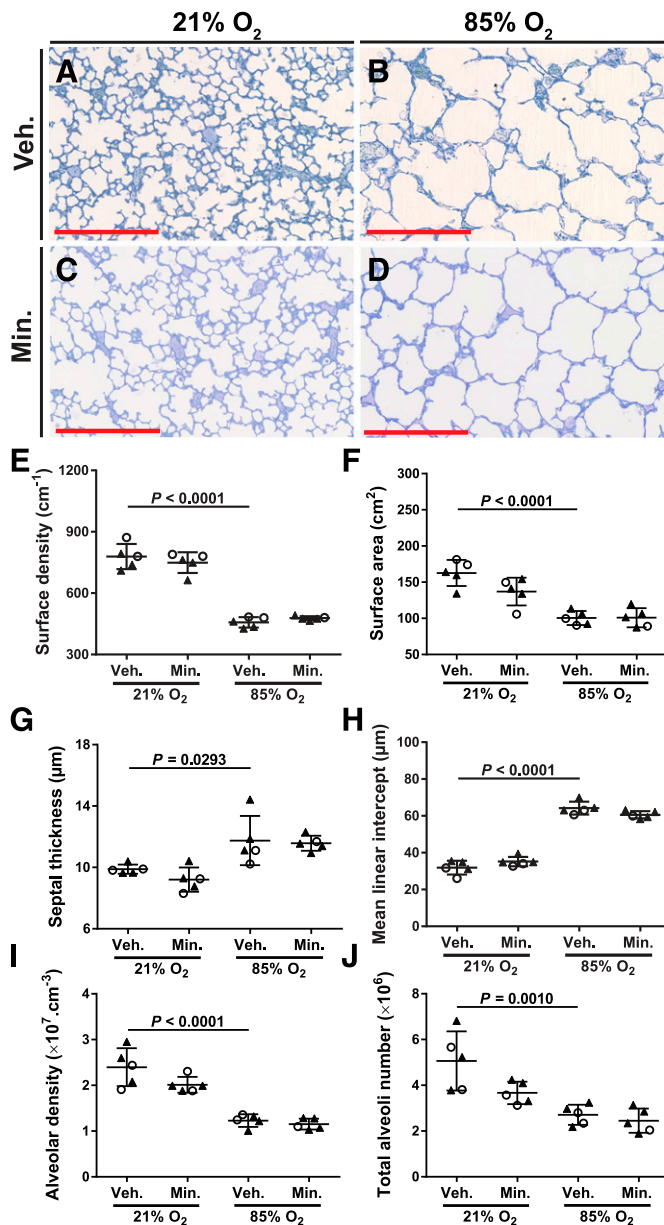


Fig. 6. Stereological analysis of mouse lung architecture. Representative sections of plastic-embedded mouse lungs from (A and B) solvent vehicle (Veh.)-treated and (C and D) minoxidil (Min.)-treated mouse pups concomitantly exposed to either (A and C) 21% O₂ or (B and D) 85% O₂. Scale bar (in red), 300 μm. The (E) gas-exchange surface density, (F) gas-exchange surface area, (G) arithmetic mean septal thickness, (H) mean linear intercept, (I) alveolar density, and (J) total alveoli number were assessed using design-based stereology. Data represent means ± S.D. ($n = 5$ experimental animals per group; each data point represents an experimental animal). Data sets were compared by one-way ANOVA with Tukey's post hoc test. Female animals are denoted by open circles, whereas male animals are denoted by closed triangles. Additional stereology parameters are provided in Table 2. Three sets of statistical comparisons are presented: one set that compares the two vehicle-treated groups (21% O₂ vs. 85% O₂), and two additional sets, each comparing the impact of minoxidil (vehicle-treated vs. minoxidil-treated) under 21% O₂ or under 85% O₂ conditions. Only the statistical comparisons in which $P < 0.05$ are presented.

decreased the mRNA transcript abundance of three cytosolic sulfotransferases and increased the abundance of another two cytosolic sulfotransferases in the lung. As it is not known which cytosolic sulfotransferases undertake the sulfation of

minoxidil in the lung, no conclusions can be made about the impact of altered expression of cytosolic sulfotransferases on minoxidil actions in the lungs.

The impact of hyperoxia on K_{ATP} channel expression in the developing lung was also addressed, since K_{ATP} channels are believed to mediate the impact of minoxidil on hair follicles and hemodynamics, and K_{ATP} channel expression is different comparing neonate versus adult rabbit myocytes (Chen et al., 1992). Hyperoxia exhibited little impact on the expression of K_{ATP} channel subunits in the lung, although differences in the expression of K_{ATP} channel subunits were noted comparing mouse pups versus adults, which is consistent with the findings reported in myocytes. Thus, the expression levels of K_{ATP} channel subunits might impact minoxidil actions in the lungs.

The authors propose that minoxidil cannot be delivered at adequate doses to the developing mouse lungs to impact lysyl hydroxylase gene expression. In Fig. 1B, the upper limit of delivery of minoxidil to the lung was 3000 ng/g wet lung tissue. To hypothetically translate that mass into a concentration in liquid, if 1 g of wet lung is equated to 1 ml of liquid, the estimated minoxidil concentration would be 0.014 mM in the sample. In the cell culture studies (Supplemental Fig. 4), 1 mM minoxidil reduced *Plod1* mRNA transcript abundance by $\sim 2\Delta CT$ (4-fold), but at 0.1 mM minoxidil, the effect was reduced to $\sim 0.5\Delta CT$ (1.4-fold). At 0.014 mM, minoxidil would be expected to be largely ineffective at reducing *Plod1* mRNA transcript abundance.

The authors have considered whether minoxidil dosing may be further optimized. Although aerosolized minoxidil administered by the inhalation route has been proposed in human adults with chronic obstructive pulmonary disease (Janssen et al., 2018), the inhalation route is not viable in newborn mouse pups. Similarly, a gavage approach has been successfully employed for the administration of minoxidil to adult mice in a model of lung fibrosis, in which minoxidil (30 mg·kg⁻¹·day⁻¹, by gavage, for 21 days) decreased expression of PLOD1, PLOD2, and PLOD3 (Shao et al., 2018). However, the gavage route is not viable in newborn mouse pups. Thus, the parenteral administration of minoxidil via the intraperitoneal route employed in the present study remained the only means of minoxidil treatment in the newborn mouse model. The plasma elimination half-life of minoxidil is ~ 4.2 hours (Canaday, 1980), whereupon minoxidil is widely distributed in tissues (Pluss et al., 1972), and accumulation in extravascular compartments explains a lengthy duration of action (Canaday, 1980). The dose of 50 mg·kg⁻¹·day⁻¹ considerably exceeds the maximum clinical pediatric dose of 1.88 mg·kg⁻¹·day⁻¹ (Puri et al., 1983) to manage hypertension in children with renal disease and was thus not considered to be too low to elicit an effect. Doses above 50 mg·kg⁻¹·day⁻¹ were not possible, as this represents the maximum possible daily dose as a result of a combination of the minoxidil stock solution solubility limit and the maximum injectable volume in newborn and neonatal mice. At a concentration of 7.5 mg·ml⁻¹, minoxidil was not soluble in water for injection. Efforts were made to improve minoxidil solubility using 10% (v/v) ethanol and 10% (v/v) DMSO; however, neither approach resulted in complete solubility of minoxidil at 7.5 mg·ml⁻¹ (Supplemental Video 1). Higher concentrations of cosolvents were not attempted, since in newborn developing rodent pups, intraperitoneal administration of 0.3 μl·g⁻¹ DMSO (Hanslick et al., 2009) or

TABLE 2

Structural parameters assessed for the lungs of mouse pups exposed to hyperoxia for the first 14 days of postnatal life, with or without minoxidil treatment, determined at postnatal day 14 by design-based stereology
Values are presented as means ± S.D., n = 5 lungs per group. One-way ANOVA with Tukey's post hoc analysis.

Parameter	21% O ₂			85% O ₂		
	Veh.		Min.	Veh.		Min.
	Mean ± S.D.	Mean ± S.D.	Mean ± S.D.	P Value vs. Veh., 21% O ₂	Mean ± S.D.	P Value vs. Veh., 85% O ₂
V (lung) (cm ³)	0.24 ± 0.025	0.22 ± 0.029	0.25 ± 0.028	0.9970	0.24 ± 0.026	0.9881
CE CV CE ² /CV ²	0.05 0.10 0.20	0.06 0.13 0.20	0.05 0.12 0.07		0.05 0.11 0.20	
V _V (par/lung) (%)	86.07 ± 0.846	84.87 ± 3.435	89.36 ± 1.129	0.0966	87.43 ± 1.849	0.4760
CE CV CE ² /CV ²	0.00 0.01 0.20	0.02 0.04 0.20	0.01 0.01 0.20		0.01 0.02 0.20	
V _V (non-par/lung) (%)	13.93 ± 0.846	15.13 ± 3.435	10.64 ± 1.129	0.0966	12.57 ± 1.849	0.4760
CE CV CE ² /CV ²	0.03 0.06 0.20	0.10 0.23 0.20	0.05 0.11 0.20		0.07 0.15 0.20	
V _V (alv air/par) (%)	61.54 ± 2.830	65.66 ± 1.306	73.25 ± 2.733	0.0001	72.34 ± 1.344	0.9096
CE CV CE ² /CV ²	0.21 0.05 0.20	0.01 0.02 0.20	0.02 0.04 0.20		0.01 0.02 0.20	
V (alv air, lung) (cm ³)	0.13 ± 0.015	0.12 ± 0.021	0.16 ± 0.016	0.0537	0.15 ± 0.020	0.8866
CE CV CE ² /CV ²	0.05 0.12 0.20	0.08 0.17 0.20	0.04 0.10 0.20		0.06 0.13 0.20	
V (sep, lung) (cm ³)	0.08 ± 0.010	0.06 ± 0.010	0.06 ± 0.011	0.0146	0.06 ± 0.007	0.9985
CE CV CE ² /CV ²	0.05 0.12 0.20	0.07 0.16 0.20	0.09 0.19 0.20		0.05 0.11 0.20	

alv, alveoli; alv air, alveolar airspaces; Min., minoxidil; non-par, nonparenchyma; par, parenchyma; sep, septa; V, volume; Veh., vehicle; V_V, volume density.

of ethanol above 1 mg·g⁻¹ (~1.3 μl·g⁻¹) (Lebedeva et al., 2017) is damaging to the development of the nervous system during the first week of postnatal life. Dimethylformamide was not attempted, since doses as low as 4 μl·g⁻¹ cause appreciable (up to 50%) mortality in adult mice (Montaguti et al., 1994), and newborn rodents are known to be more sensitive to dimethyl formamide than are adults (<https://hpvchemicals.oecd.org/UI/handler.axd?id=558b5269-b0ef-46a7-b240-b07c066ad62f>). In sum, these data suggest that minoxidil administered at 50 mg·kg⁻¹·day⁻¹ via the intraperitoneal route cannot be used to limit lysyl hydroxylase activity during postnatal mouse lung development. These findings underscore the need 1) for the development of lysyl hydroxylase assays that can be performed in complex biological (organ homogenate) samples and 2) for the identification of specific chemical inhibitors of lysyl hydroxylases. Indeed, efforts to identify new small-molecular inhibitors of lysyl hydroxylase 2 using high-throughput screening are already underway (Devkota et al., 2019) and will hopefully provide an alternative to minoxidil in the future.

Authorship Contributions

Participated in research design: Pfeffer, Lignelli, Inoue, Mižíková, Surate Solaligue, Steenbock, Myti, Vadász, Herold, Seeger, Brinckmann, Morty.

Conducted experiments: Pfeffer, Lignelli, Inoue, Mižíková, Surate Solaligue, Steenbock, Myti.

Contributed new reagents or analytic tools: Vadász, Herold, Seeger, Brinckmann, Morty.

Performed data analysis: Pfeffer, Lignelli, Inoue, Mižíková, Surate Solaligue, Steenbock, Myti, Vadász, Herold, Seeger, Brinckmann, Morty.

Wrote or contributed to the writing of the manuscript: Pfeffer, Lignelli, Myti, Brinckmann, Morty.

References

Albertine KH, Jones GP, Starcher BC, Bohnsack JF, Davis PL, Cho SC, Carlton DP, and Bland RD (1999) Chronic lung injury in preterm lambs. Disordered respiratory tract development. *Am J Respir Crit Care Med* **159**:945–958.
Alejandre-Alcázar MA, Kwapiszewski G, Reiss I, Amarie OV, Marsh LM, Sevilla-Pérez J, Wygrecka M, Eul B, Köbrich S, Hesse M, et al. (2007) Hyperoxia modulates TGF-β/BMP signaling in a mouse model of bronchopulmonary dysplasia. *Am J Physiol Lung Cell Mol Physiol* **292**:L537–L549.
Allali-Hassani A, Pan PW, Dombrowski L, Najmanovich R, Tempel W, Dong A, Loppnau P, Martin F, Thornton J, Edwards AM, et al. (2007) Structural and

chemical profiling of the human cytosolic sulfotransferases [published correction appears in *PLoS Biol* (2007) 5:e165]. *PLoS Biol* **5**:e97.
Alnouti Y and Klaassen CD (2006) Tissue distribution and ontogeny of sulfotransferase enzymes in mice. *Toxicol Sci* **93**:242–255.
Baeuerle PA and Huttner WB (1986) Chlorate—a potent inhibitor of protein sulfation in intact cells. *Biochem Biophys Res Commun* **141**:870–877.
Bank RA, Robins SP, Wijmenga C, Breslau-Siderius LJ, Bardoe AF, van der Sluijs HA, Pruijs HE, and TeKoppele JM (1999) Defective collagen crosslinking in bone, but not in ligament or cartilage, in Bruck syndrome: indications for a bone-specific telopeptide lysyl hydroxylase on chromosome 17. *Proc Natl Acad Sci U S A* **96**:1054–1058.
Bland RD, Xu L, Ertsey R, Rabinovitch M, Albertine KH, Wynn KA, Kumar VH, Ryan RM, Swartz DD, Csiszar K, et al. (2007) Dysregulation of pulmonary elastin synthesis and assembly in preterm lambs with chronic lung disease. *Am J Physiol Lung Cell Mol Physiol* **292**:L1370–L1384.
Branchfield K, Li R, Lungova V, Verheyden JM, McCulley D, and Sun X (2016) A three-dimensional study of alveogenesis in mouse lung. *Dev Biol* **409**:429–441.
Brinckmann J, Kim S, Wu J, Reinhardt DP, Batmunkh C, Metzen E, Notbohm H, Bank RA, Krieg T, and Hunzelmann N (2005) Interleukin 4 and prolonged hypoxia induce a higher gene expression of lysyl hydroxylase 2 and an altered cross-link pattern: important pathogenetic steps in early and late stage of systemic sclerosis? *Matrix Biol* **24**:459–468.
Buhl AE, Waldon DJ, Baker CA, and Johnson GA (1990) Minoxidil sulfate is the active metabolite that stimulates hair follicles. *J Invest Dermatol* **95**:553–557.
Canaday B (1980) Minoxidil. *South Med J* **73**:59–64.
Cardinale GJ and Udenfriend S (1974) Prolyl hydroxylase. *Adv Enzymol Relat Areas Mol Biol* **41**:245–300.
Chen F, Wetzel GT, Friedman WF, and Klitzner TS (1992) ATP-sensitive potassium channels in neonatal and adult rabbit ventricular myocytes. *Pediatr Res* **32**:230–235.
Chen Y, Terajima M, Yang Y, Sun L, Ahn YH, Pankova D, Puperi DS, Watanabe T, Kim MP, Blackmon SH, et al. (2015) Lysyl hydroxylase 2 induces a collagen cross-link switch in tumor stroma. *J Clin Invest* **125**:1147–1162.
Devkota AK, Veloria JR, Guo HF, Kurie JM, Cho EJ, and Dalby KN (2019) Development of a high-throughput lysyl hydroxylase (LH) assay and identification of small-molecule inhibitors against LH2. *SLAS Discov* **24**:484–491.
Eisinger-Mathason TS, Zhang M, Qiu Q, Skuli N, Nakazawa MS, Karakasheva T, Mucaj V, Shay JE, Stangenberg L, Sadri N, et al. (2013) Hypoxia-dependent modification of collagen networks promotes sarcoma metastasis. *Cancer Discov* **3**:1190–1205.
Gjaltema RA and Bank RA (2017) Molecular insights into prolyl and lysyl hydroxylation of fibrillar collagens in health and disease. *Crit Rev Biochem Mol Biol* **52**:74–95.
Gottlieb TB, Katz FH, and Chidsey CA III (1972) Combined therapy with vasodilator drugs and beta-adrenergic blockade in hypertension. A comparative study of minoxidil and hydralazine. *Circulation* **45**:571–582.
Hanslick JL, Lau K, Noguchi KK, Olney JW, Zorumski CF, Mennerick S, and Farber NB (2009) Dimethyl sulfoxide (DMSO) produces widespread apoptosis in the developing central nervous system. *Neurobiol Dis* **34**:1–10.
Hautala T, Heikkinen J, Kivirikko KI, and Myllylä R (1992) Minoxidil specifically decreases the expression of lysine hydroxylase in cultured human skin fibroblasts. *Biochem J* **283**:51–54.
Hsia CC, Hyde DM, Ochs M, and Weibel ER; ATS/ERS Joint Task Force on Quantitative Assessment of Lung Structure (2010) An official research policy statement of the American Thoracic Society/European Respiratory Society: standards for quantitative assessment of lung structure. *Am J Respir Crit Care Med* **181**:394–418.
Ichida M, Fujita C, Sumie R, Miyano R, and Inoue H (2020) Simultaneous determination of minoxidil and minoxidil sulfate by high-performance liquid chromatography with UV-detection and its applications. *Med Drug Discov* **7**:100050.
Jackson JC, Clark JG, Standaert TA, Truog WE, Murphy JH, Juul SE, Chi EY, and Hodson WA (1990) Collagen synthesis during lung development and during

- hyaline membrane disease in the nonhuman primate. *Am Rev Respir Dis* **141**: 846–853.
- Janssen R, Piscoer I, and Wouters EF (2018) Inhalation therapy for repairing damaged elastin fibers and decelerating elastinolysis in chronic obstructive pulmonary disease. *Expert Rev Respir Med* **12**:349–360.
- Kasamatsu A, Uzawa K, Hayashi F, Kita A, Okubo Y, Saito T, Kimura Y, Miyamoto I, Oka N, Shiiba M, et al. (2019) Deficiency of lysyl hydroxylase 2 in mice causes systemic endoplasmic reticulum stress leading to early embryonic lethality. *Biochem Biophys Res Commun* **512**:486–491.
- Kivirikko KI and Prockop DJ (1972) Partial purification and characterization of procollagen lysine hydroxylase from chick embryos. *Biochim Biophys Acta* **258**: 366–379.
- Krane SM, Pinnell SR, and Erbe RW (1972) Lysyl-procollagen hydroxylase deficiency in fibroblasts from siblings with hydroxylysine-deficient collagen. *Proc Natl Acad Sci USA* **69**:2899–2903.
- Kumarasamy A, Schmitt I, Nave AH, Reiss I, van der Horst I, Dony E, Roberts JD Jr, de Krijger RR, Tibboel D, Seeger W, et al. (2009) Lysyl oxidase activity is dysregulated during impaired alveolarization of mouse and human lungs. *Am J Respir Crit Care Med* **180**:1239–1252.
- Lambert JF, Benoit BO, Colvin GA, Carlson J, Delville Y, and Quesenberry PJ (2000) Quick sex determination of mouse fetuses. *J Neurosci Methods* **95**:127–132.
- Lebedeva J, Zakharov A, Ogievetsky E, Minlebaeva A, Kurbanov R, Gerasimova E, Sitdikova G, and Khazipov R (2017) Inhibition of cortical activity and apoptosis caused by ethanol in neonatal rats *in vivo*. *Cereb Cortex* **27**:1068–1082.
- Lignelli E, Palumbo F, Myti D, and Morty RE (2019) Recent advances in our understanding of the mechanisms of lung alveolarization and bronchopulmonary dysplasia. *Am J Physiol Lung Cell Mol Physiol* **317**:L832–L887.
- Mariani TJ, Sandefur S, and Pierce RA (1997) Elastin in lung development. *Exp Lung Res* **23**:131–145.
- Mecham RP (2012) Overview of extracellular matrix. *Curr Protoc Cell Biol* **Chapter 10**:Unit10 11.
- Mecham RP (2018) Elastin in lung development and disease pathogenesis. *Matrix Biol* **73**:6–20.
- Messenger AG and Rundegren J (2004) Minoxidil: mechanisms of action on hair growth. *Br J Dermatol* **150**:186–194.
- Mizíková I and Morty RE (2015) The extracellular matrix in bronchopulmonary dysplasia: target and source. *Front Med (Lausanne)* **2**:91.
- Mizíková I, Palumbo F, Tábi T, Herold S, Vadász I, Mayer K, Seeger W, and Morty RE (2017) Perturbations to lysyl oxidase expression broadly influence the transcriptome of lung fibroblasts. *Physiol Genomics* **49**:416–429.
- Mizíková I, Pfeffer T, Nardiello C, Surate Solaligue DE, Steenbock H, Tatsukawa H, Silva DM, Vadász I, Herold S, Pease RJ, et al. (2018) Targeting transglutaminase 2 partially restores extracellular matrix structure but not alveolar architecture in experimental bronchopulmonary dysplasia. *FEBS J* **285**:3056–3076.
- Mizíková I, Ruiz-Camp J, Steenbock H, Madurga A, Vadász I, Herold S, Mayer K, Seeger W, Brinckmann J, and Morty RE (2015) Collagen and elastin cross-linking is altered during aberrant late lung development associated with hyperoxia. *Am J Physiol Lung Cell Mol Physiol* **308**:L1145–L1158.
- Montaguti P, Melloni E, and Cavalletti E (1994) Acute intravenous toxicity of dimethyl sulfoxide, polyethylene glycol 400, dimethylformamide, absolute ethanol, and benzyl alcohol in inbred mouse strains. *Arzneimittelforschung* **44**:566–570.
- Murad S and Pinnell SR (1987) Suppression of fibroblast proliferation and lysyl hydroxylase activity by minoxidil. *J Biol Chem* **262**:11973–11978.
- Murad S, Tennant MC, and Pinnell SR (1992) Structure-activity relationship of minoxidil analogs as inhibitors of lysyl hydroxylase in cultured fibroblasts. *Arch Biochem Biophys* **292**:234–238.
- Myllylä R, Wang C, Heikkinen J, Juffer A, Lampela O, Risteli M, Ruotsalainen H, Salo A, and Sipilä L (2007) Expanding the lysyl hydroxylase toolbox: new insights into the localization and activities of lysyl hydroxylase 3 (LH3). *J Cell Physiol* **212**: 323–329.
- Nardiello C, Mizíková I, Silva DM, Ruiz-Camp J, Mayer K, Vadász I, Herold S, Seeger W, and Morty RE (2017) Standardisation of oxygen exposure in the development of mouse models for bronchopulmonary dysplasia. *Dis Model Mech* **10**: 185–196.
- Nave AH, Mizíková I, Niess G, Steenbock H, Reichenberger F, Talavera ML, Veit F, Herold S, Mayer K, Vadász I, et al. (2014) Lysyl oxidases play a causal role in vascular remodeling in clinical and experimental pulmonary arterial hypertension. *Arterioscler Thromb Vasc Biol* **34**:1446–1458.
- Northway WH Jr, Rosan RC, and Porter DY (1967) Pulmonary disease following respirator therapy of hyaline-membrane disease. Bronchopulmonary dysplasia. *N Engl J Med* **276**:357–368.
- Piersma B and Bank RA (2019) Collagen cross-linking mediated by lysyl hydroxylase 2: an enzymatic battlefield to combat fibrosis. *Essays Biochem* **63**:377–387.
- Pinnell SR and Murad S (1987) Effects of minoxidil on cultured human skin fibroblasts. *Dermatologica* **175** (Suppl 2):12–18.
- Pluss RG, Orcutt J, and Chidsey CA (1972) Tissue distribution and hypotensive effects of minoxidil in normotensive rats. *J Lab Clin Med* **79**:639–647.
- Puri HC, Maltz HE, Kaiser BA, and Potter DE (1983) Severe hypertension in children with renal disease: treatment with minoxidil. *Am J Kidney Dis* **3**:71–75.
- Rein G, Glover V, and Sandler M (1982) Multiple forms of phenolsulphotransferase in human tissues: selective inhibition by dichloronitrophenol. *Biochem Pharmacol* **31**: 1893–1897.
- Reiter C and Weinshilboum RM (1982) Acetaminophen and phenol: substrates for both a thermostable and a thermolabile form of human platelet phenol sulfotransferase. *J Pharmacol Exp Ther* **221**:43–51.
- Ruiz-Camp J, Quantius J, Lignelli E, Arndt PF, Palumbo F, Nardiello C, Surate Solaligue DE, Sakkas E, Mizíková I, Rodríguez-Castillo JA, et al. (2019) Targeting miR-34a/Pdgfra interactions partially corrects alveologenesis in experimental bronchopulmonary dysplasia. *EMBO Mol Med* **11**:e9448.
- Ruotsalainen H, Sipilä L, Vapala M, Sormunen R, Salo AM, Uitto L, Mercer DK, Robins SP, Risteli M, Aszodi A, et al. (2006) Glycosylation catalyzed by lysyl hydroxylase 3 is essential for basement membranes. *J Cell Sci* **119**:625–635.
- Schindelin J, Arganda-Carreras I, Frise E, Kaynig V, Longair M, Pietzsch T, Preibisch S, Rueden C, Saalfeld S, Schmid B, et al. (2012) Fiji: an open-source platform for biological-image analysis. *Nat Methods* **9**:676–682.
- Schittny JC (2017) Development of the lung. *Cell Tissue Res* **367**:427–444.
- Shao S, Zhang X, Duan L, Fang H, Rao S, Liu W, Guo B, and Zhang X (2018) Lysyl hydroxylase inhibition by minoxidil blocks collagen deposition and prevents pulmonary fibrosis via TGF- β /Smad3 signaling pathway. *Med Sci Monit* **24**: 8592–8601.
- Takaluoma K, Hyry M, Lantto J, Sormunen R, Bank RA, Kivirikko KI, Myllyharju J, and Soininen R (2007) Tissue-specific changes in the hydroxylysine content and cross-links of collagens and alterations in fibril morphology in lysyl hydroxylase 1 knock-out mice. *J Biol Chem* **282**:6588–6596.
- Thibeault DW, Mabry SM, Ekekezie II, Zhang X, and Truog WE (2003) Collagen scaffolding during development and its deformation with chronic lung disease. *Pediatrics* **111**:766–776.
- Todaro GJ and Green H (1963) Quantitative studies of the growth of mouse embryo cells in culture and their development into established lines. *J Cell Biol* **17**:299–313.
- Van Slyke DD and Hiller A (1921) An unidentified base among the hydrolytic products of gelatin. *Proc Natl Acad Sci USA* **7**:185–186.
- Witsch TJ, Niess G, Sakkas E, Likhoshvay T, Becker S, Herold S, Mayer K, Vadász I, Roberts JD Jr, Seeger W, et al. (2014a) Transglutaminase 2: a new player in bronchopulmonary dysplasia? *Eur Respir J* **44**:109–121.
- Witsch TJ, Turowski P, Sakkas E, Niess G, Becker S, Herold S, Mayer K, Vadász I, Roberts JD Jr, Seeger W, et al. (2014b) Deregulation of the lysyl hydroxylase matrix cross-linking system in experimental and clinical bronchopulmonary dysplasia. *Am J Physiol Lung Cell Mol Physiol* **306**:L246–L259.
- Zappacosta AR (1980) Reversal of baldness in patient receiving minoxidil for hypertension. *N Engl J Med* **303**:1480–1481.
- Zhou Y, Horowitz JC, Naba A, Ambalavanan N, Atabai K, Balestrini J, Bitterman PB, Corley RA, Ding BS, Engler AJ, et al. (2018) Extracellular matrix in lung development, homeostasis and disease. *Matrix Biol* **73**:77–104.
- Zins GR (1988) The history of the development of minoxidil. *Clin Dermatol* **6**: 132–147.
- Zuurmond AM, van der Slot-Verhoeven AJ, van Dura EA, De Groot J, and Bank RA (2005) Minoxidil exerts different inhibitory effects on gene expression of lysyl hydroxylase 1, 2, and 3: implications for collagen cross-linking and treatment of fibrosis. *Matrix Biol* **24**:261–270.

Address correspondence to: Rory E. Morty, Department of Lung Development and Remodelling, Max Planck Institute for Heart and Lung Research, Parkstrasse 1, 61231 Bad Nauheim, Germany. E-mail: rory-morty@mpi-bn.mpg.de

Online supplement to

Minoxidil cannot be used to target lysyl hydroxylases during post-natal mouse lung development: a cautionary note

Tilman Pfeffer, Ettore Lignelli, Hajime Inoue, Ivana Mižíková, David E. Surate Solaligue, Heiko Steenbock, Despoina Myti, István Vadász, Susanne Herold, Werner Seeger, Jürgen Brinckmann, and Rory E. Morty

This online supplement consists of the legends for **Supplemental Video S1**, and **Supplemental Figures S1-S5**, as well as the artwork of **Supplemental Figures S1-S5**.

Video S1. The solubility of minoxidil at $7.5 \text{ mg}\cdot\text{ml}^{-1}$ in water for injection, 10% (v/v) ethanol, and 10% (v/v) dimethylsulfoxide (DMSO) is illustrated by pipetting.

Fig. S1. Uncropped immunoblots from Fig. 3. The full uncropped blots presented in Fig. 3 are provided: **(A)** the initial blot developed after probing for PLOD1, and **(B)** the second blot developed after the PLOD1 blot in **(A)** was re-probed for β -actin.

Fig. S2. Steady-state mRNA transcript abundance of cytosolic sulfotransferases. **(A)** The steady-state mRNA transcript abundance of cytosolic transferases *Sult1a1*, *Sult1c1*, *Sult1c2*, *Sult1d1*, *Sult5a1*, and *Sult5a1* was determined by real-time RT-PCR in mRNA extracts from the lungs of mouse pups exposed either to 21% O₂ (blue closed circles) or 85% O₂ (orange closed squares) for the first 14 days of postnatal life. Data reflect mean $\Delta\text{CT} \pm \text{S.D}$ ($n=3$ mice per group). Statistical comparisons were made using a one-way ANOVA with a Tukey's *post hoc* test. **(B)** *Sult1b1*, *Sult1e1*, and *Sult2a1* were not detected in mRNA from mouse lungs, however, could be detected in mRNA from the mouse liver, gut, or testis. N.D., not detected.

Fig S3. Steady-state mRNA transcript abundance of K_{ATP} subunits. The steady-state mRNA transcript abundance of mRNA encoding the pore-forming K_{ATP} subunits *Kcnj8* and *Kcnj11*, and the sulfonylurea receptor subunits *Abcc8* and *Abcc9* were profiled using real-time RT-PCR in mRNA extracts from the lungs of mouse pups exposed either to 21% O₂ (blue closed circles) or 85% O₂ (orange closed squares) for the first 14 days of postnatal life, as well as from adult (three month old) mouse lungs (closed green triangles). Data reflect mean $\Delta\text{CT} \pm \text{S.D}$ ($n=3$ mice per group). Statistical comparisons were made using a one-way ANOVA with a Tukey's *post hoc* test.

Fig. S4. Steady-state mRNA transcript abundance of *Plod1*, *Plod2*, and *Plod3* in NIH/3T3 cells treated with minoxidil or minoxidil sulfate. The steady-state mRNA transcript abundance of *Plod1*, *Plod2*, and *Plod3* mRNA were profiled using real-time RT-PCR in mRNA extracts from NIH/3T3 cells treated with vehicle (V, water for injection), or minoxidil (M) or minoxidil sulfate (MS) at concentrations of either 0.1 mM or 1.0 mM. Data reflect mean $\Delta\text{CT} \pm \text{S.D}$ ($n=3$ samples per group, each sample consisting of a pool of two wells of separate cultures). Statistical comparisons were made using a one-way ANOVA with a Tukey's *post hoc* test.

Fig. S5. Steady-state mRNA transcript abundance of *Plod1*, *Plod2*, and *Plod3* in NIH/3T3 cells treated with pharmacological modulators of cytosolic sulfotransferase pathway enzymes. The steady-state mRNA transcript abundance of *Plod1*, *Plod2*, and *Plod3* mRNA transcripts were profiled using real-time RT-PCR in mRNA extracts from NIH/3T3 cells treated with vehicle (V, water for injection), 50 mM sodium chlorate (C), 5 mM acetaminophen (A), or 1 μM 2,4-dichloro-6-nitrophenol (D) for 1 h, prior to the addition of 1 mM minoxidil (M). CM, AM, and DM reflect a combination of the respective compound with minoxidil. The dashed line represents the position of the minoxidil alone bar, presented in Fig. S4. Data reflect mean $\Delta\text{CT} \pm \text{S.D}$ ($n=3$ samples per group, each sample consisting of a pool of two wells of separate cultures).

Fig. S1

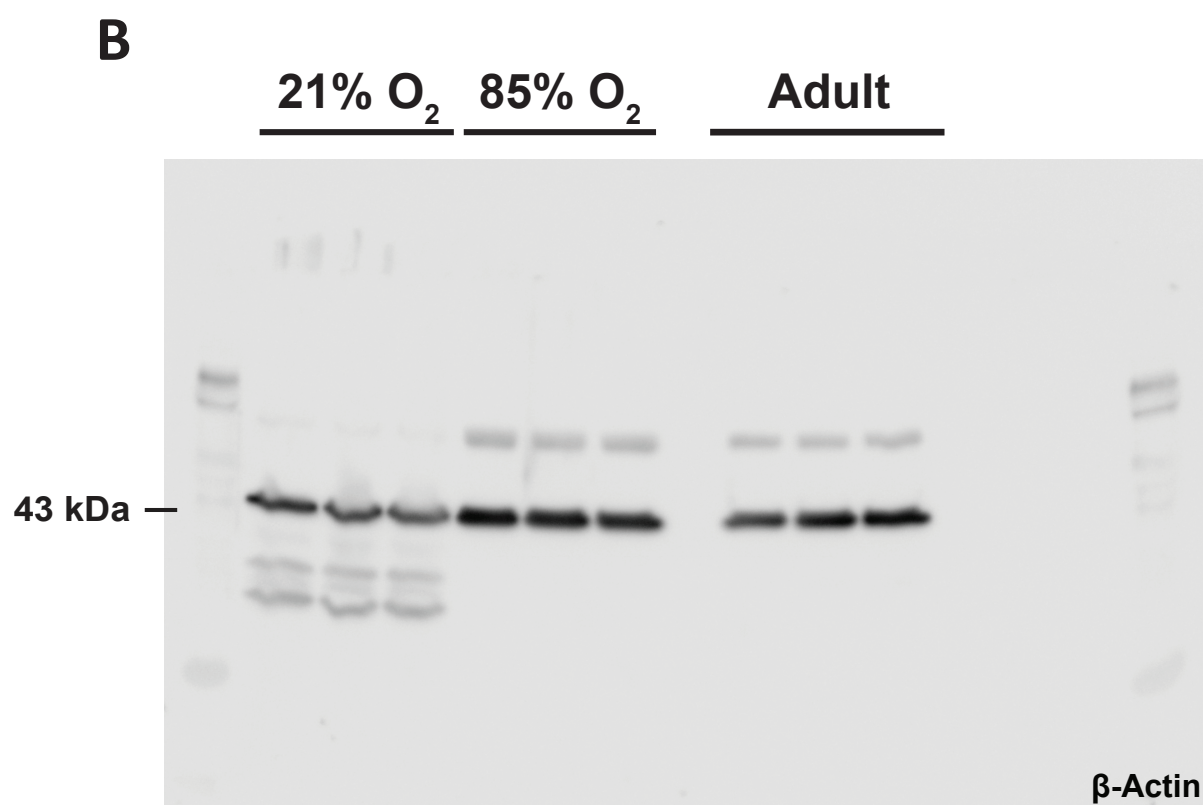
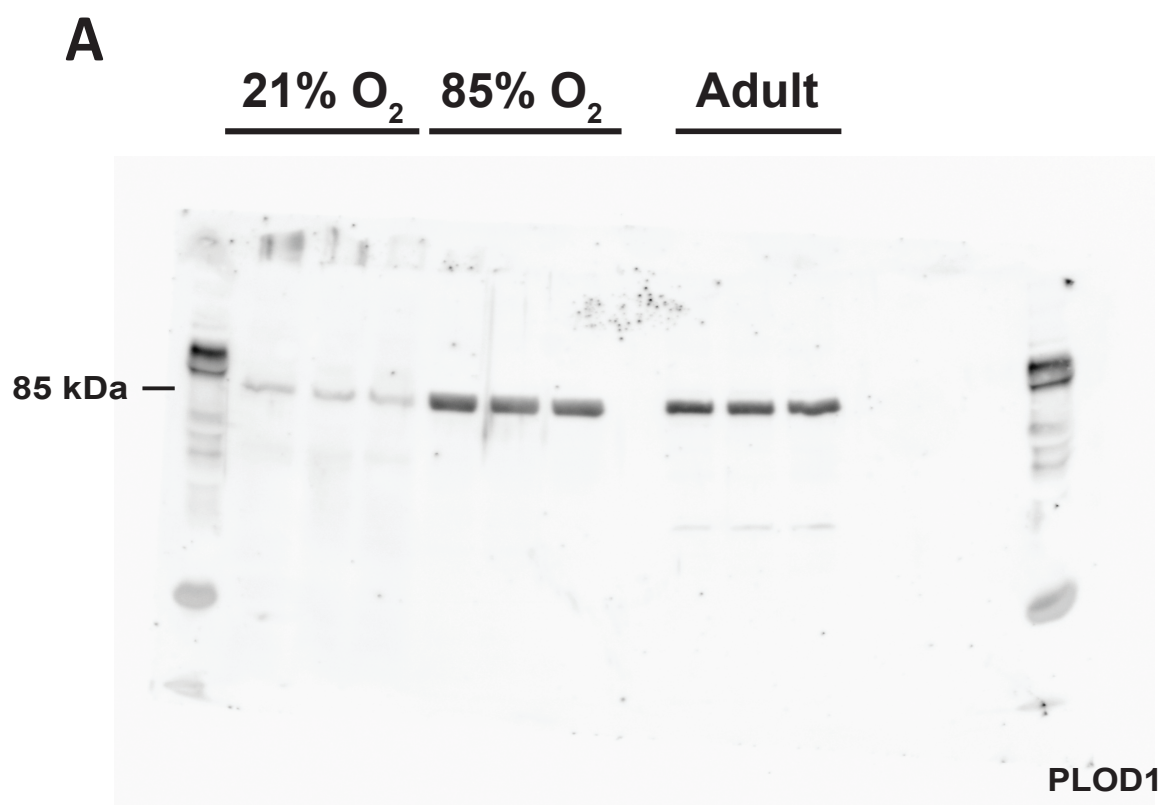
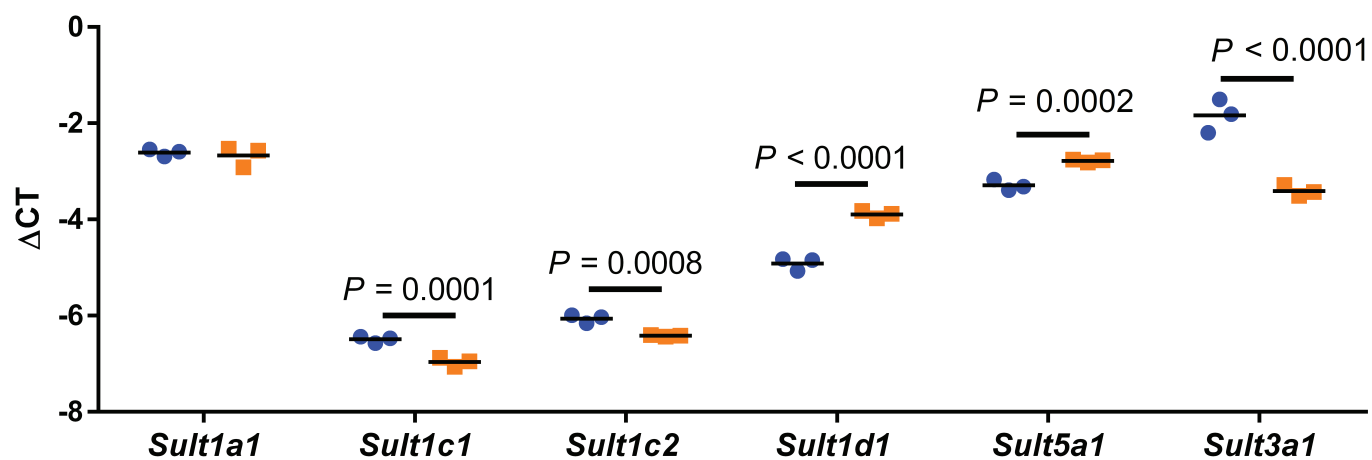


Fig. S2

A



B

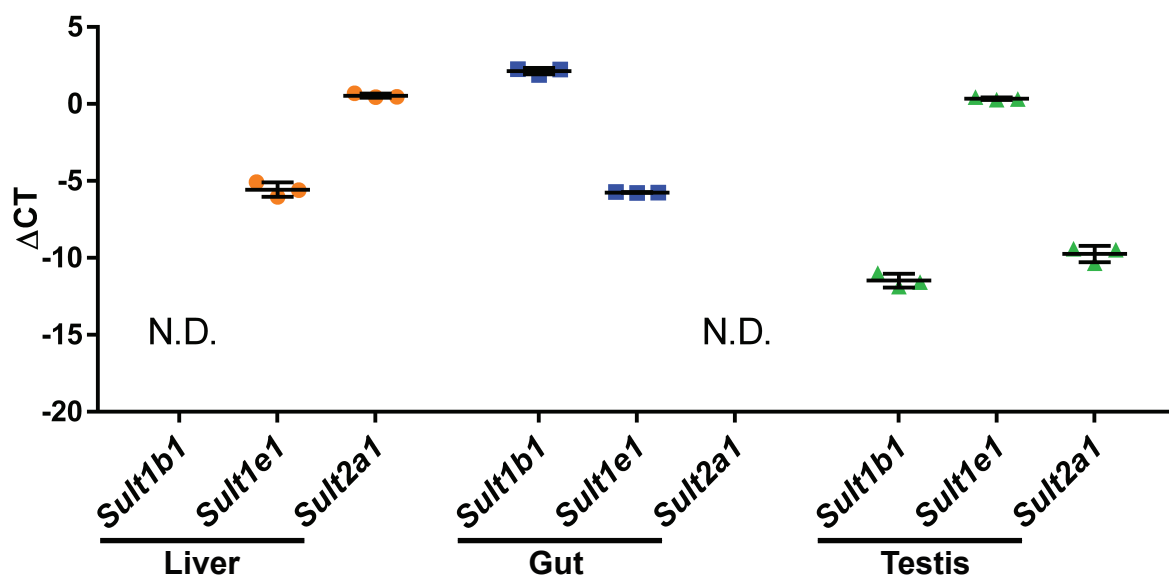


Fig. S3

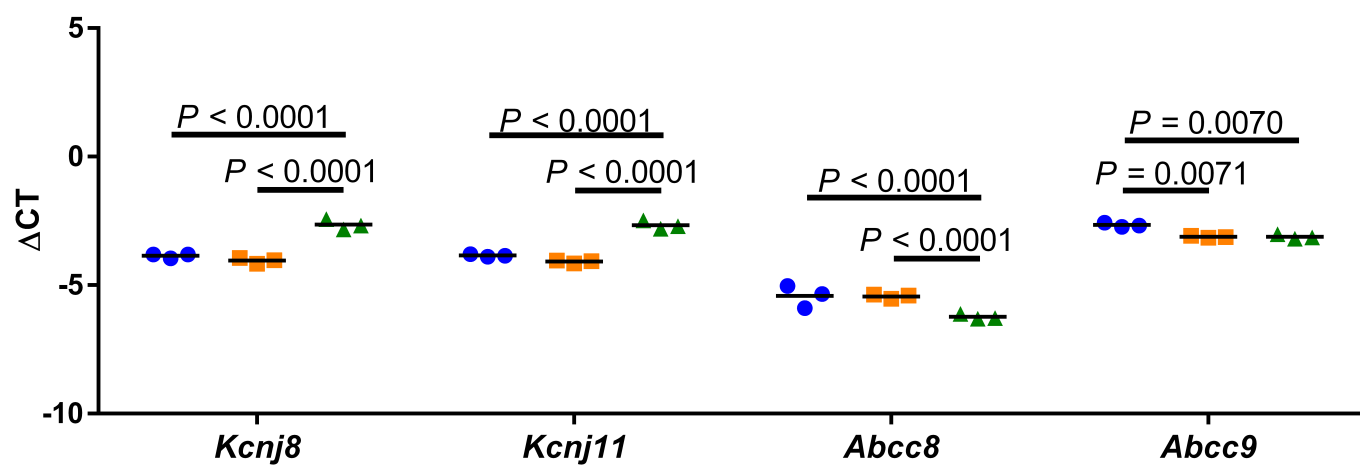


Fig. S4

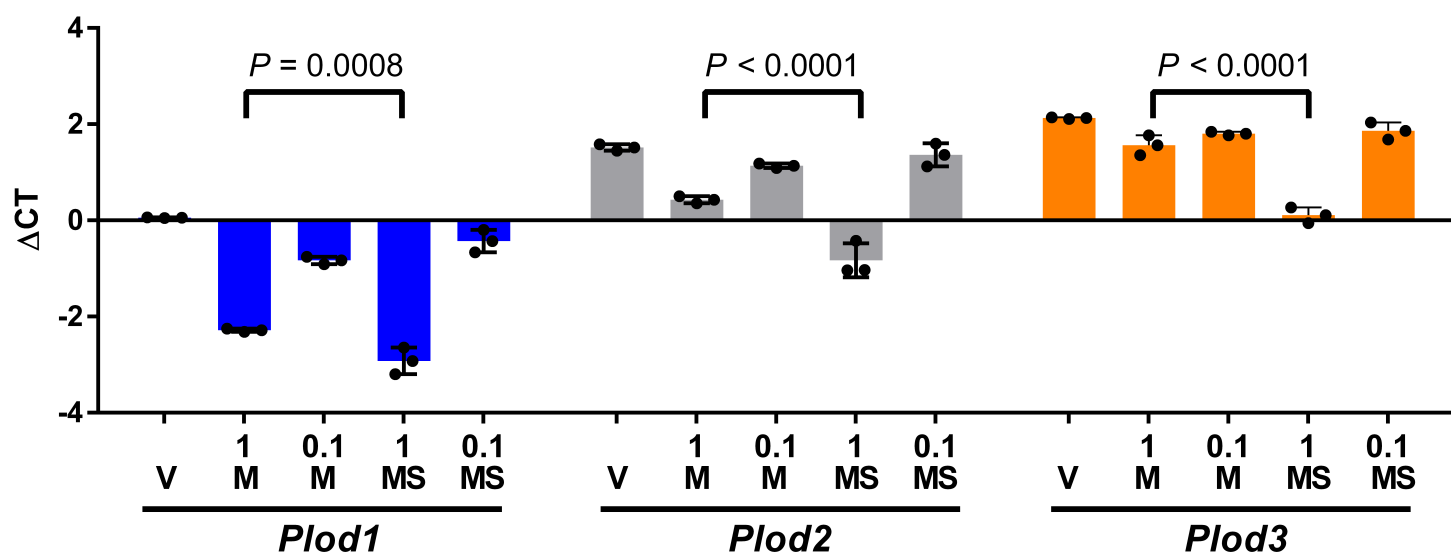


Fig. S5

